SOILS AND FOUNDATIONS Vol. 43, No. 4, 131–147, August 2003
Japanese Geotechnical Society

# TIME-DEPENDENT BEHAVIOUR OF OIL RESERVOIR CHALK: A MULTIPHASE APPROACH

V. DE GENNARO[i], P. DELAGE[i], Y.-J. CUI[i], CH. SCHROEDER[ii] and F. COLLIN[ii]

## ABSTRACT

In the North Sea Ekofisk oilfield, oil is located in a 300 m thick layer of porous chalk ($n=40$–$50\%$) at a 3000 m depth. After the initial phase of depletion an enhanced oil recovery procedure was carried out by injecting sea water (waterflooding). An unexpected consequence of this waterflooding has been the occurrence of a seafloor subsidence, corresponding up to now to a decrease of the seafloor level of approximately 10 m. It is now well recognised that hydro-mechanical coupling involving multiphase fluid interactions (oil and water) is determinant for the interpretation of the phenomenological aspects associated with the chalk compaction and the related subsidence observed in the North Sea oilfields (Ekofisk reservoir) when water flooded. The subsidence due to waterflooding is interpreted as a collapse phenomenon due to suction decrease, typical of loose and low plasticity unsaturated soils when wetted under load. On the other hand, time-dependent stress-strain behaviour of geomaterials is one of the major concerns in soil mechanics and, in effect, subsidence includes creep effects. A multiphase approach, including creep effects under controlled suction levels, is proposed in this paper; the preliminary results of this study are presented and discussed. Attention will be focused at first on the theoretical approach, supplying the essential elements for the work, and on the interpretation of the experimental results. This will provide secondly the base for formulation and validation of the constitutive law proposed for the description of the time-dependent mechanical behaviour of the chalk.

**Key words:** constitutive modelling, creep, multiphase chalk, oil-water suction, osmotic technique, overpressure technique, subsidence, time-dependent behaviour (**IGC**: F4/F5/G13)

## INTRODUCTION

The seafloor subsidence observed in the North Sea oilfields since the eighties is related to the starting of the assisted oil recovery by sea waterflooding. The total amount of the settlement of the seafloor observed up to now is of about 10 m, with a subsidence rate of nearly 0.4 m per year (Nagel, 2001). This settlement is due to the reduction in thickness of the 300 m thick chalk layer located at a 3000 m depth below the seafloor. It has constituted a significant economic problem since the oil operators have been obliged to elevate the operating offshore platforms to a corresponding height, resulting in significant extra costs and revision of production strategy (Hermansen et al., 2000).

The subsidence due to waterflooding in reservoir chalks is a coupled problem typical of a multiphase geomaterial, i.e. the chalk full of water and of oil. In a previous paper (Delage et al., 1996), it was shown how this problem could be considered within a framework taken from the mechanics of unsaturated soils. By considering oil as a non wetting phase (like air in unsaturated soils) and water as a wetting fluid (like in unsaturated soils), it was demonstrated that the volume reduction under waterflooding could be interpreted as a collapse phenomenon. Also, the Barcelona Basic Model (BBM) (Alonso et al., 1990) was successfully used to qualitatively model the complete hydromechanical history of the chalk deposit. This approach was confirmed later by the Pasachalk EC project, by running an experimental program in which the oil-water suction $s=u_o-u_w$ (where $u_o$ and $u_w$ are the oil and water pressures respectively) was controlled. To do so, the independent control of both pressures with $u_o>u_w$ was achieved, resulting in a positive value of the suction (Pasachalk, 2000). In this regard, experimental observation allowed extending the concept of capillary pressure, in which only oil-water-chalk capillary actions are considered, to that of suction, which also includes the various existing physico-chemical chalk-water interactions. The approach was also quantitatively confirmed by using a constitutive model derived from the BBM model, called Pasachalk model, that was implemented in a finite elements code. Satisfactory results were obtained in modelling laboratory waterflooding tests and also a simplified chalk reservoir configuration (Charlier et al., 2002; Collin et al., 2002).

[i] CERMES, Ecole Nationale des Ponts et Chaussées-LCPC, 6 et 8 avenue Blaise Pascal-Cité Descartes, Champs-sur-Marne 77455, Marne-la-Vallée Cedex 2-France (degennar@cermes.enpc.fr).
[ii] Department GéomaC (University of Liége), Liége, Belgium.
Manuscript was received for review on July 31, 2002.
Written discussions on this paper should be submitted before March 1, 2004 to the Japanese Geotechnical Society, Sugayama Bldg. 4F, Kanda Awaji-cho 2-23, Chiyoda-ku, Tokyo 101-0063, Japan. Upon request the closing date may be extended one month.

To better interpret the subsidence that has occurred in the chalk deposit since the eighties, it was also planned to account for time-dependent effects, that are supposed to be significant in chalks (Andersen et al., 1992; Gutierrez and Kolderup, 1999). More precisely, it was decided to investigate in the laboratory the time-dependent behaviour of chalk samples containing two fluids (oil and water) under controlled oil-water suction conditions. This approach, which is complementary to standard investigations already carried out with only one fluid (water or oil, among others: Newman, 1983; Ruddy et al., 1989; Piau and Maury, 1994; Andersen, 1995; Krogsbøll, 1997; Papamichos et al., 1997; Schroeder et al., 1998; Risnes et al., 1999; Homand and Shao, 2000), seems indispensable to better account for the real problem in the reservoir. To the authors knowledge, such creep tests under constant oil-water suction do not seem to have been previously published in the literature. This paper presents the specific experimental methods developed to carry out these tests, with a particular emphasis given to the relevant strain rate to adopt. Also, some previous experimental results showing some aspects of the time-dependent behaviour of a reservoir chalk under a controlled suction are given and interpreted in the framework of existing knowledge on the time-dependent behaviour of geomaterials. Finally, a constitutive model derived from the Perzyna (1964) approach is developed and some previous modelling is presented.

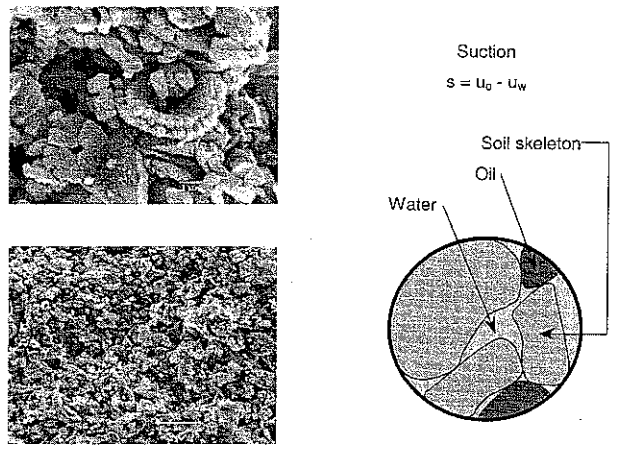


**Fig. 1. SEM images of Lixhe chalk at various magnifications and simplified scheme of oil-water-chalk interactions**

## MATERIALS AND METHODS

In order to investigate the time-dependent behaviour of oil reservoir chalks, a preliminary series of isotropic triaxial compression tests under controlled suction condition (drained test) has been performed. Since the basic idea of Pasachalk project was that the mechanical response of chalk saturated by water (wetting fluid) and oil (non wetting fluid) can be interpreted in the same way as for the mechanical behaviour of unsaturated soils (where water is the wetting fluid and air is the non wetting fluid), emphasis is put on the definition of the retention properties of the chalk in terms of the $s - S_{rw}$ relationship and suction control.

### *Chalk Tested*

Chalk is essentially made up of skeletal debris of unicellular algae (coccolithes), these coccolithes are often non-articulated grains, which are crystals of calcite. The average grain size ranges from 2 $\mu$m to 10 $\mu$m. Due to the costs of field plugs, it is common to perform tests on outcrop chalks. The major shortcoming, however, is that outcrop chalks have never been in contact with oil, and this may have some important implications for the definition of the overall behaviour of the material.

All the tests presented in this paper have been carried out on outcrop chalk coming from the CBR quarry near the town of Visé (Belgium), also called Lixhe chalk. The microstructure of Lixhe chalk is very close to that of many North Sea Chalks, this is the major reason justifying the choice of this chalk in this study. The remains of coccolithes are present in small plates of about 1 to 10 microns dimensions (SEM picture, Fig. 1(a)). Between the calcite grains, the voids (dimensions 1 to 5 microns) represent about the half of the total volume, with an average porosity of about 40%. This value of porosity was corroborated by a series of mercury porosimeter tests, the latter allowed to identify a monodispersed family of major pores having an average radius of about 0.37 $\mu$m. In the quarry deposit, voids are generally filled with water in chemical equilibrium with the chalk (saturated in $CaCO_3$), whereas the porous network of the reservoir chalk is generally filled with water and oil. Previous investigations on this material allowed quantification of values of the intrinsic permeability of about $1 \times 10^{-14}$ m$^2$ ($k_{water} \cong 1 \times 10^{-8}$ ms$^{-1}$, $k_{oil} \cong 7 \times 10^{-9}$ ms$^{-1}$). The oil used in this study is a non polar organic liquid (Soltrol 170®, Phillips Petroleum Company), it does not contain any polycyclic aromatic hydrocarbons so it is not toxic. Furthermore, Soltrol 170 has been chosen also for its very low solubility in water ($\ll 1$ mg/l at 20°C) and volatility in air ($\ll 4 \times 10^{-2}$ mm$^3/h$ at 20°C), and because it is non water miscible. Characteristic numbers for Soltrol 170 are: dynamic viscosity $\eta_{oil} = 2.028$ cP, fluid density $\rho_{oil} = 0.78$ Mg m$^{-3}$.

### *Suction Control: Osmotic and Overpressure Techniques*

In a porous medium, the contact between two non miscible fluids induces a discontinuity of the values of pressure through the interface separating the two fluids. This discontinuity is also called capillary pressure (Laplace, 1806; quoted by Morrow, 1970). In the context of thermodynamics, capillary pressure is only a component of a more general potential energy, introduced in geomechanics since the early sixties, called "suction". The latter involves the surface energetic related to the system fluids (water and oil) and to the solid-fluid systems (oil-solid and water-solid) (Fig. 1(b)). Indeed, at a microscopic level, the suction is the result of complex physico-chemical interactions, among which is the capil-

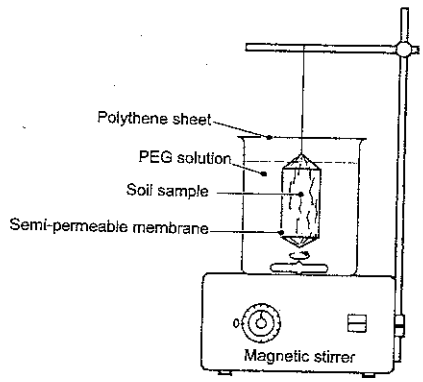


**Fig. 2. Schematic layout of the apparatus for suction control via osmotic technique (after Cui and Delage, 1996)**

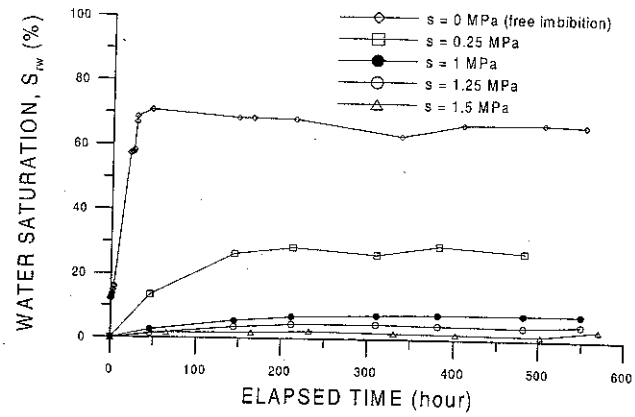


**Fig. 3. Imbibition curves of Lixhe chalk at various suction levels**

lary effect. Due to the key role played by suction on the behaviour of chalk, experimentation required a set of testing procedures allowing for the control of suction. Two techniques have been used in this study:

—the osmotic technique;

—the overpressure method, allowing for the independent control of both fluid pressures with $u_o > u_w$, resulting in $s = u_o - u_w > 0$.

Osmotic technique

The osmotic technique is rarely used in unsaturated soils, and apparently never used in petroleum engineering. It was used successfully by Kassiff and Benshalom (1971) and extensively developed for unsaturated soil testing by Delage and co-workers (Delage et al., 1992; Cui and Delage, 1996). The technique is based on the osmotic principle. The difference between two solutions having different concentrations and separated by a semi-permeable membrane induces a difference between the pressures of the two solutions, this difference is the osmotic pressure. This technique can be applied to a soil sample containing air and water. A partially saturated sample is inserted and sealed in a tube-shaped cellulotic semi-permeable membrane characterised by a specific value of MWCO (Molecular Weight Cut Off). The membrane containing the sample is then immersed in an aqueous solution of big sized molecules of polyethylene glycol (PEG), the whole system is at atmospheric pressure (Fig. 2). Since PEG molecules can not cross the semi-permeable membrane, the difference between the concentration of PEG solution ($c_{peg}$) and of interstitial water ($c_w$), with $c_{peg} > c_w$, will induce a passage of water from the soil sample, through the membrane, into the solution. However, an antagonistic mechanism is associated with the reduction of water content of the sample, since pore water pressure decreases and a certain amount of water will pass from the solution into the sample. At the end of a period of equalisation, the system will tend to equilibrium under the induced actions due to the differences in concentration and pressure. Suction is then applied to the water through the membrane by osmosis and its value is controlled by the concentration of the solution: higher PEG concentrations provide higher suctions (Williams and Shaykewich, 1969; Delage et al., 1998).

The osmotic technique has been adopted in this study in order to control the oil-water suction $s = u_o - u_w$ in chalk, in view of the determination of the retention properties of the tested material. Having been used essentially for the experimentation on water partially saturated soils, first, a verification of the resistance of the special semi-permeable membrane (Spectra/Por® 12000–14000 Daltons MWCO, Spectrum Laboratories Inc.) to the contact of oil was necessary. This preliminary investigation provided satisfactory results, enabling the use of this technique for controlling suction during some tests on chalk full of oil and water. As shown in Fig. 2, a magnetic stirrer is used in order to improve the exchange kinetic of water and ensure the homogeneity of the PEG solution. A plastic film (polythene sheet) is used in order to reduce the evaporation of the solution, so as to have a constant concentration in PEG. The value of $c_{peg}$ is obtained by measuring the refractive Brix index (Br) of the PEG solution, the corresponding value of suction $s$ is obtained from the following relationship (Delage et al., 1998):

$$s = \left(\frac{Br\sqrt{11}}{90 - Br}\right)^2. \quad (1)$$

Suction equalisation is related to the evolution of the weight of the soil sample, which is progressively wetted until stabilisation at the water content value corresponding to the suction level imposed. The weight and dimension changes of the sample are then systematically monitored and values are then used to calculate the corresponding degree of water saturation $S_{rw}$; depending on the nature of soil and the dimensions of the sample, time for weight stabilisation can vary between 1 and 5 weeks.

Figure 3 shows the imbibition curves of Lixhe chalk obtained with the osmotic technique. The characteristics of the samples used in the experimentation are summarised in Table 1. Chalk sample has been prepared following a standard preparation procedure, namely: oven dried at 105°C, oil saturated under vacuum (−94 kPa during 24 hours), and wetted (osmotic technique) in order to attain the desired value of suction. Actually, during oil production, the same process is involved: oil is pushed

**Table 1. Physical properties of chalk samples (osmotic technique)**

| Sample | A | B | C | D | E |
|---|---|---|---|---|---|
| Suction, $s$ (MPa) | 0.00 | 0.25 | 1.00 | 1.25 | 1.50 |
| Diameter (mm) | 29.63 | 29.45 | 30.12 | 29.17 | 29.68 |
| Height (mm) | 36.84 | 36.98 | 34.88 | 39.80 | 36.00 |
| $V_t$ (cm$^3$) | 25.40 | 25.19 | 24.86 | 26.59 | 24.90 |
| $V_s$ (cm$^3$) | 14.69 | 15.63 | 15.24 | 16.37 | 14.24 |
| $V_v$ (cm$^3$) | 10.71 | 9.56 | 9.61 | 10.22 | 10.66 |
| $e$ | 0.73 | 0.61 | 0.63 | 0.62 | 0.75 |
| $n$ | 0.42 | 0.38 | 0.39 | 0.38 | 0.43 |
| $w_{res}$ | 0.17 | 0.86 | 1.21 | 0.82 | 0.24 |
| $S_{rw}$ (%) | 0.64 | 3.74 | 5.11 | 3.49 | 0.85 |

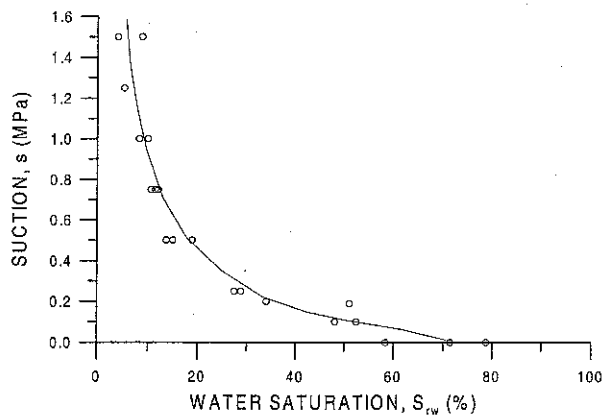


**Fig. 4. Water retention curve of Lixhe chalk (wetting path)**

out of the porous network by water injection (waterflooding), and the chalk deposit is submitted to a water imbibition process. As can be inferred from the results in Fig. 3, the exchange kinetic is a function of the suction level applied. The higher the suction gradient, the slower is the exchange kinetic. From the plateau of the imbibition curves in Fig. 3, a final value of $S_{rw}$ can be obtained, corresponding to a given level of imposed suction. The relationship between $s$ and $S_{rw}$ can be established plotting the couple of points $s-S_{rw}$, as shown in Fig. 4. These points are fitted by a well defined curve, which gives the retention curve for Lixhe chalk under a wetting path. As can be noted, at low suction levels, chalk is quite prone to water saturation (maximum $S_{rw} \cong 80\%$ when $s=0$), this reflects the general tendency of this material to be water-wet rather than oil-wet.

It is worth observing that at high suction levels, a variation of 50% of suction (for instance: from 1 MPa to 0.5 MPa) is associated with small changes in drained water volume (about 10%, $S_{rw}$ changes from 10% to 20%, Fig. 4), whereas for lower suction levels, the void volume affected by the same variation of suction is two times higher.

Overpressure technique

The overpressure technique is probably the most used technique to control suction in unsaturated soils. It allows imposing the values of suction by working in the positive range of pressures. This is obtained by increasing simultaneously the values of pressure of the wetting fluid (water) and non-wetting fluid (oil in this study), translating the pressure of the wetting fluid in the positive range. The use of a small pore sized ceramic porous stone permits imposing two different pressures on the two fluids saturating the porous sample (Richards, 1941). Independent control of both oil and water pressures is then possible, allowing for a wide range of suction control. The first well documented application of this technique for unsaturated soil testing comes from Bishop and Donald (1961), who developed a special triaxial apparatus allowing performance of suction controlled tests on loose silts. An equalisation stage is required in order to stabilise water and oil volume exchanges from and to the sample under the suction target imposed in terms of oil and water pressures. In order to assess the end of the equalisation phase, it is common practice to account for the stabilisation of the total volume and the water volume of the sample, or alternatively to assume a limit value of water content change rate (e.g. Mancuso et al., 2002).

*Triaxial Testing Device and Procedure*

Triaxial tests under suction control were carried out in a high pressure, auto-compensated triaxial cell Geodesign® (Fig. 5(a)). The auto-compensation acts in the axial direction, and is related to the action of the confining pressure on the axial piston. A connection between the confining chamber and the auto-compensation chamber allows application of the same pressure in opposite direction on equal surfaces (surfaces A and B in Fig. 5(a)). Consequently, during deviatoric tests, the force applied by the piston in the axial direction gives purely the deviator stress. The cell is servo-controlled by means of four volume-pressure controllers (GDS) connected to a data acquisition-piloting system (Fig. 5(b)). Two GDS with a maximum capacity of 64 MPa are used to apply the confining pressure and the deviator stress, respectively.

The overpressure technique allows the control of suction during the test. Oil and water pressures are applied via two GDS, with a maximum capacity of 3 MPa. The first GDS applies the oil pressure ($u_o$) through two bronze porous stones. The first porous stone is placed at the top of the sample, the second one is part of the composite base pedestal at the bottom of the sample (Fig. 5(b)). The central part of the composite base pedestal incorporates a high air entry value ceramic porous stone connected to the second GDS used for the application of water pressure ($u_w$). This ceramic porous stone permits a free movement of water through it, while the oil (as a non wetting fluid) can not cross it if its pressure does not exceed the capillary pressure value $p_c$ of the ceramic porous stone.

Strain measurements are obtained locally, by means of a special frame mounted around the chalk sample and equipped with 5 LVDTs (Linear Variable Differential Transformers). Details of this frame are given in Fig. 5(b). It consists of three independent rigid rings, equally spaced in the axial direction, fixed around the sample by means of three high stiffness springs oriented at 120° in the radial direction. Note that the frame is

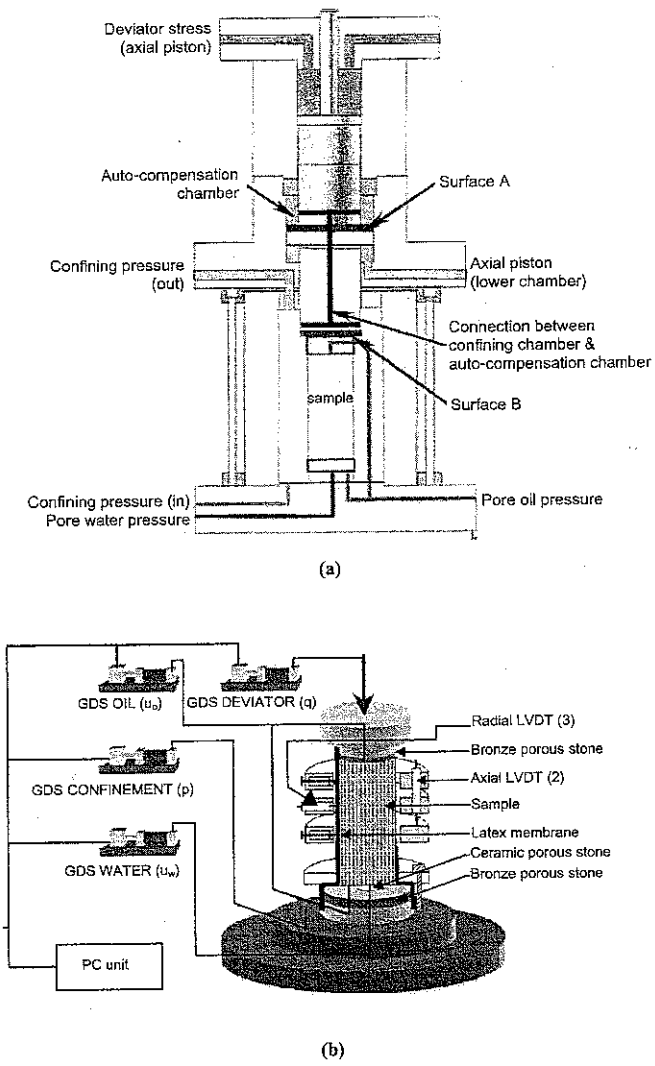


**Fig. 5. The auto-compensated triaxial cell: (a) schematic layout of the apparatus and (b) acquisition/piloting system and local measurements system**

positioned at the middle of the height of the sample, consequently LVDT measurements are virtually insensitive to the effect of sample ends. The average axial strain is obtained by means of two axial LVDT (25 mm range) fixed to the upper ring on the diameter of the sample. They measure the relative displacement between the upper and the lower ring. The average radial strain is calculated via 3 LVDT (5 mm range) oriented at 120° in the radial direction and mounted on the middle ring shown in Fig. 5(b).

All the chalk samples tested have initial dimensions of about 38 mm in diameter and 76 mm in height. They were extracted from a block of outcrop chalk, taking care that all samples had the same orientation, machined on lathe, then oven dried during 24 hours at 105°C and finally oil saturated under vacuum (−94 kPa during 24 hours). In order to impose the selected suction level and to reduce time for equalisation in the triaxial cell, samples were pre-equilibrated out of the cell using the osmotic technique. When equilibrium was reached, samples were transferred inside the cell and the suction level was re-established by means of the two GDS controllers. The specimens were mounted with filter papers at both ends and over the cylindrical surface in order to have maximum drainage surface and a more homogeneous suction distribution. Finally, samples were submitted to the selected testing programme.

*Loading Rates*

Experimental and theoretical approaches in time-dependent stress-strain behaviour of geomaterials is one of the major concerns in soil mechanics (e.g., Richardson and Whitman, 1963; Bjerrum, 1967; Singh and Mitchell, 1968; Adachi and Oka, 1982; Janbu, 1985; Tatsuoka et al., 2000). It has long been recognised that the choice of the appropriate stress and/or strain rate during mechanical tests on saturated fine grained soils (i.e. silts, clays) is essential in order to avoid excess pore-water pressure generation and to apply fully effective stresses to the sample (Gibson and Henkel, 1954). Suggested values of controlled axial displacement during triaxial tests on London clay ($k \cong 1 \times 10^{-9}$ m s$^{-1}$) are of about 0.25 $\mu$m/min. On the other hand, there is experimental evidence that increased testing times in less sensitive plastic and soft clays induce important reduction in undrained shear strength and preconsolidation pressure, together with indications of time dependency of yield envelopes (Graham et al., 1983). Leroueil et al. (1985), in a detailed study presented on the compressibility of natural clays, indicated that stress-strain-strain rate relationship for these materials is unique. In particular, it was found that preconsolidation stress-strain rate relation is independent of the test conditions (constant rate of strain test or creep test) and that at a given strain, the higher the strain rate, the higher is the effective stress (and the preconsolidation pressure).

In partially saturated soils, in order to ensure suction control, the loading rate should be small enough to allow free water mass exchange (Ho and Fredlund, 1982; Delage et al., 1987). Values of about 1 $\mu$m/min of axial displacement rate are considered adequate in order to avoid unsuited variations of suction.

All the tests presented have been run following a load controlled procedure. On the existing literature there are not enough data related to the admissible loading rates in chalks. Axial strain rates of about $0.1\%/h$ (i.e. $2.7 \times 10^{-7}$ s$^{-1}$) have been used on almost fully oil-saturated chalks ($S_{rw} \cong 5\%$) and reputed to be slow enough to avoid excess oil-pressure generation (Havmøller and Foged, 1998). Deviator loading rates of about $1.6 \times 10^{-4}$ MPa s$^{-1}$ have been applied during triaxial tests at constant confining pressure in order to prevent excess pore pressure (Homand and Shao, 2000). Based on previous findings, two isotropic loading rates have been retained in this study, namely: $3.3 \times 10^{-3}$ MPa/s (fast rate) and $5.5 \times 10^{-5}$ MPa /s (slow rate). Hereinafter we will use exclusively the terms "slow rate" and "fast rate". Obviously this is a crucial point of the experimentation, as previously pointed out. In this respect, it is worth mentioning that fluid mass exchanges and overpressure during load-controlled tests are essentially linked to the loading induced volu-

Table 2. Physical properties and testing conditions of chalk samples (triaxial cell)

| Sample | Height (mm) | Diameter (mm) | $V_t$ (cm$^3$) | $V_s$ (cm$^3$) | $V_v$ (cm$^3$) | $W_s$ (g) | $e_o$ | $n_o$ | $W_{sat\text{-}oil}$ (g) | $S_{r\text{-}oil}$ (%) | $S_{rw}$ (%) Osmotic | $S_{rw}$ (%) Overpressure | $\Delta S_{rw}$ (%) | Suction, $s$ (kPa) | Comments | $p_{creep}$ (MPa) |
|---|---|---|---|---|---|---|---|---|---|---|---|---|---|---|---|---|
| T1 | 75.56 | 37.95 | 85.47 | 53.09 | 32.37 | 141.76 | 0.610 | 0.379 | 166.91 | 99.94 | 58.96 | 57.18 | (−)1.78 | 0 | Isotropic test | 30 |
| | | | | | | | | | | | | | | | Fast rate | |
| T2 | 76.39 | 37.96 | 86.45 | 53.21 | 33.25 | 142.06 | 0.625 | 0.385 | 167.24 | 99.55 | 17.35 | 18.77 | (+)1.42 | 200 | Isotropic test | 15 |
| | | | | | | | | | | | | | | | 1st loading slow rate /Creep/ | 24.9 |
| | | | | | | | | | | | | | | | 2nd loading slow rate /Creep/ | 49.9 |
| | | | | | | | | | | | | | | | 3rd loading fast rate /Creep/ | |
| T3 | 72.5 | 37.8 | 81.36 | 48.91 | 32.45 | 130.58 | 0.664 | 0.399 | 150.61 | 96.61 | 21.43 | 20.35 | (−)1.08 | 500 | Isotropic test | No creep |
| | | | | | | | | | | | | | | | Fast rate | |
| T4 | 75.86 | 37.83 | 85.27 | 50.14 | 35.13 | 133.87 | 0.701 | 0.412 | 160.90 | 99.77 | 10.35 | 10.32 | (−)0.03 | 1000 | Isotropic test | 50 |
| | | | | | | | | | | | | | | | 1st loading slow rate /Unloading/ | |
| | | | | | | | | | | | | | | | 2nd loading fast rate /Creep/ | |
| T5 | 75.97 | 37.88 | 85.62 | 50.37 | 35.24 | 134.49 | 0.700 | 0.412 | 161.80 | 99.89 | 2.45 | 3.60 | (+)1.15 | 1000 | Isotropic test | 22 |
| | | | | | | | | | | | | | | | Fast rate | 50 |

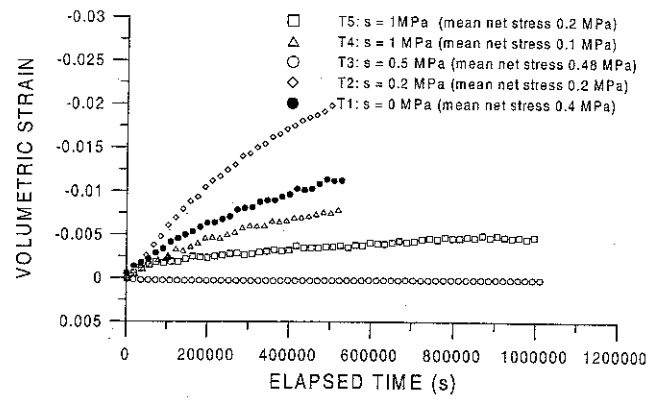


**Fig. 6. Volumetric strain evolution during equalisation (overpressure technique)**

metric strain rates. The aim of this paper is to discuss these relevant aspects of the time-dependent mechanical behaviour of partially and multiphase saturated chalks under the specific condition of controlled suction.

## EXPERIMENTAL RESULTS

Five triaxial isotropic compression tests under suction control have been performed in this study. The testing conditions of each sample are summarised in Table 2 tests have been conducted in such a way as to collect the larger amount of information with respect to two specific factors, namely: suction dependency and time dependency (loading rate and creep). To this aim, we have performed initial loading phases at slow rate or fast rate up to yield, followed by successive phases of creep, during which the mean total stress was maintained constant, and then reloading at fast or slow rate (cf. Table 2). All the samples were submitted to a preliminary equalisation stage, in order to bring them to the corresponding level of imposed suction.

*Equalisation Stage*

Due to the larger dimensions of chalk samples tested in the triaxial apparatus with respect to the samples used for the determination of the imbibition curve of Lixhe chalk (cf. Tables 1 and 2), time for suction equalisation was expected to be very long. For that reason, it was decided to adopt a mixed solution, allowing for a first equalisation by osmosis followed by a final equalisation, inside the triaxial cell, using the overpressure technique. Results of the equalisation stages for all the samples are presented in Figs. 6 and 7. During the process, values of mean net stress ($p_{net} = p - u_o$) were kept constant and small enough to avoid excessive compression of the specimens. As can be inferred, samples undergo swelling (Fig. 6) and water content increase (Fig. 7). Equalisation was stopped when changes in water content of the samples, as given by the GDS controller of water, were negligible over the time scale of the process (from 1 week to 11 days). This is directly readable from the curve trends shown in Fig. 7, where evolution of the water volume versus time is dis-

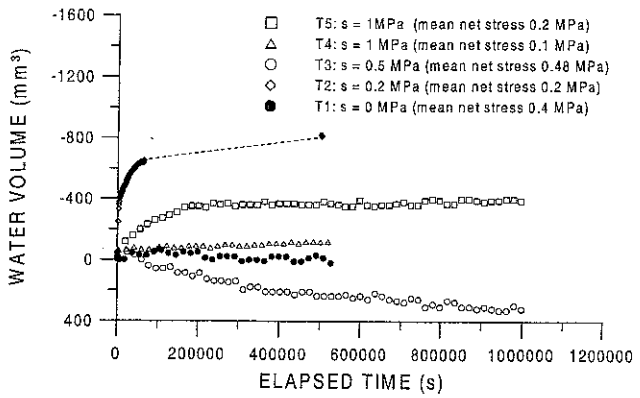


**Fig. 7. Water volume evolution during equalisation (overpressure technique)**

played (negative values are conventionally referred to water volume moving out of the GDS). From the curves presented in Figs. 6 and 7, these is no obvious indication to delineate a possible ordered trend with respect to suction. Indeed, rather than suction dependency, it is believed that curves shown in these figures mostly characterise the different final partial saturation (in oil and water) attained for each sample at the end of the preliminary equalisation stage by osmosis. It is likely that the increase of the sample and water volumes (as shown in Figs. 6 and 7) is merely the consequence of further adjustments of the sample set-up, once the system is mounted into the cell and submitted to the three independent pressures, namely: the confining pressure ($p$), the oil pressure ($u_o$) and the water pressure ($u_w$). Thus, it is important to verify whether the two techniques for suction control (osmosis and overpressure) give same results in terms of $s - S_{rw}$ relationship. To this scope, the values of $S_{rw}$ at the end of the equalisation by osmotic technique are compared in Table 2 to those obtained at the end of the overpressure equalisation stage in triaxial cell. Values are deduced taking into account data shown in Figs. 6 and 7. The results indicate a satisfactory compatibility between the two techniques, with a maximum variation of $S_{rw}$ of about 1.8% (sample T1).

*Isotropic Compression*

Figure 8 shows the loading programme imposed for each of the tested chalk specimens. As mentioned, increasing confining pressure up to yield was applied at slow and fast rate, excepting test T3 ($s = 0.5$ MPa), for which an intermediate loading rate has been assumed.

Isotropic compression test results are presented in Fig. 9. Within the natural variability of the outcrop block porosity, two main "families" of void ratios are distinguishable, namely: $e_o \cong 0.6$ (denser samples) and $e_o \cong 0.7$ (looser samples). Both suction effects and loading rate effects are discernible: at a given suction, the higher the loading rate, the higher is the mean total stress at yield (e.g. tests T4 and T5) and the stiffer is the elastic response of the material. The effect of the loading rate is quite evident by considering the results of tests T1 and T2.

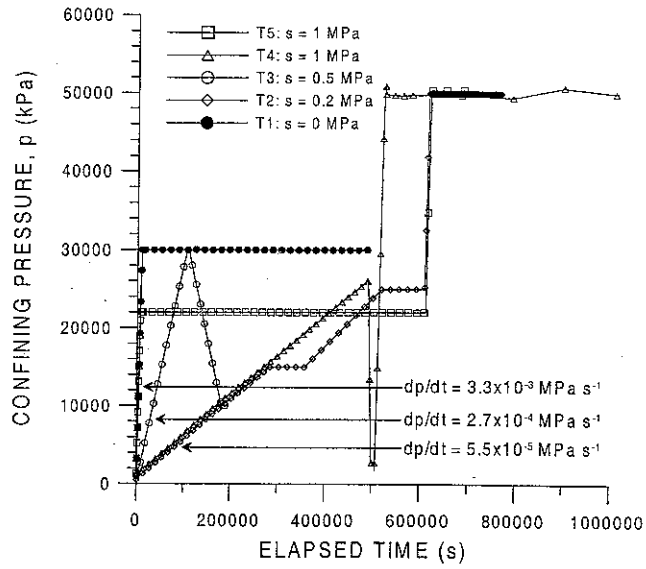


**Fig. 8. Isotropic triaxial compression tests on chalk: loading programme**

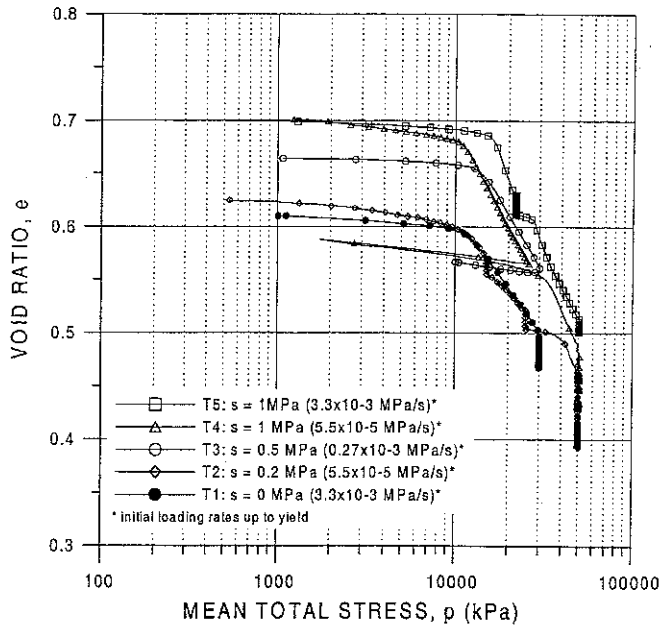


**Fig. 9. Isotropic triaxial compression curves of Lixhe chalk at various suction levels**

Irrespective of the difference of suction levels, the difference between these two curves is small and it seems reasonable to associate that with the higher loading rate imposed during test T1. On the other hand, increasing suction induces a progressive passage from a "water-like" behaviour to a "oil-like" behaviour. Generally, this corresponds to a stiffer response in the elastic regime (e.g. tests T1 and T5), an increase of the mean total stress at yield and a more pronounced transition from elastic to elastoplastic regime when yield occurs. These observation are summarised in Figs. 10 and 11 in terms of bulk modulus values and mean total stress values at yield, respectively. In this respect, we draw reader's attention to the

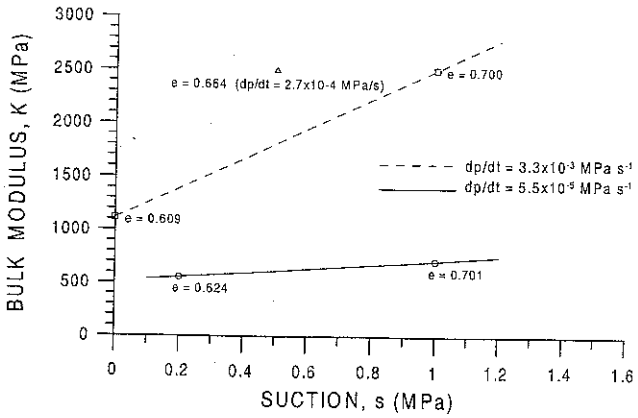


**Fig. 10. Variation in bulk modulus with suction and loading rates**

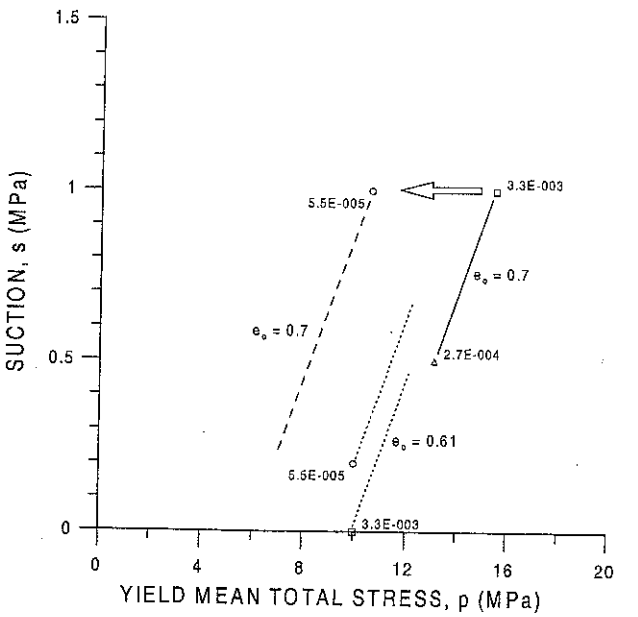


**Fig. 11. Variation of mean total stress at yield (preconsolidation stress) with suction and loading rates**

influence of the porosity on the test results. In fact, from past experimental results (Pasachalk, 2000), the difference in mean total stress at yield between the two extreme limits of "oil-like" state (tests T4 and T5, $s=1$ MPa) and "water-like" state (test T1, $s=0$ MPa) should be more pronounced than what is observed (about 6 MPa, cf. Fig. 11). Unfortunately, samples at low suction levels are also the denser, hence suction effects are partially hidden by the increasing stiffness due to the reduced compressibility of the material.

*Loading Rate Dependent Behaviour and Suction Effects*

Since no measurements of water and oil pore pressures were performed during the tests, some conjectures arise as to whether all these tests can be considered fully drained or not depending on the loading rate. Clearly, being that the magnitude of undissipated pore-fluid pressures (i.e. oil and water pressures) are controlled by the permeability and the compressibility of the chalk and the

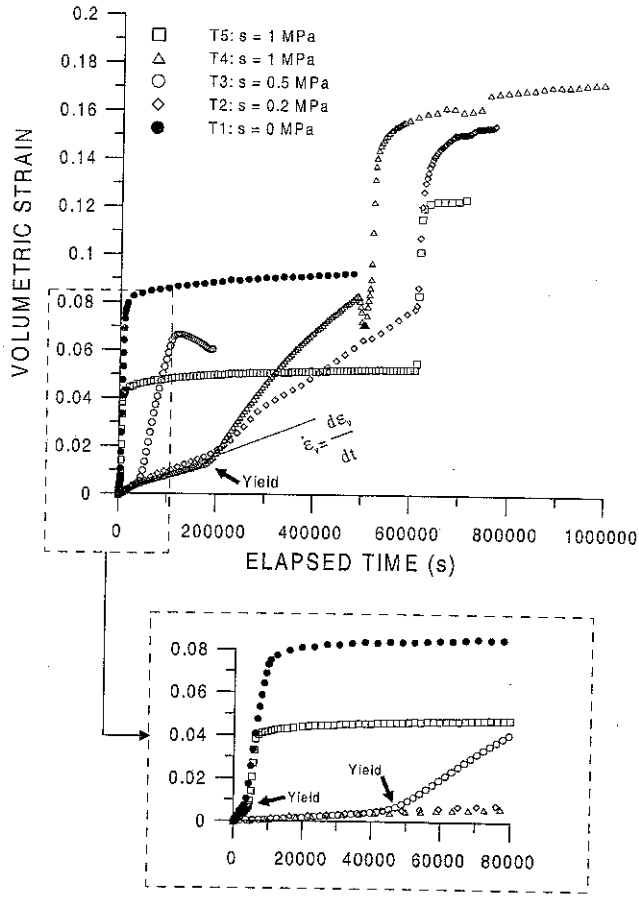


**Fig. 12. Evolution of volumetric strain during isotropic tests on chalk at various loading rates**

loading rate, the amount of stresses applied to the sample may be very different. Following the general approach typical for unsaturated soils, two independent stress variables describe the mechanical behaviour of water and oil saturated chalk, namely: the mean net stress $p_{net}=p-u_o$ and the oil-water suction $s=u_o-u_w$. Consequently, if excess pore pressures are supposed to develop, being that $u_o>0$, this will induce reduced values of applied mean net stress $p_{net}$, and higher values of mean total stress necessary for yielding. However, based on the definition of oil-water suction, excess pore-fluid pressure will affect the value of imposed suction, depending on the degree of saturation of chalk in both fluids. In that case, it is believed that various factors could affect significantly the process of excess pore pressure generation and dissipation, resulting in an overall variation of the suction level before the re-establishment of the initial constant value. Among these factors let us quote: fluid viscosity, surface wettability, continuity of the fluid phases, the existence of bulk water (low suction) or menisci-water (high suction).

In a first attempt to verify the dependency of the tests upon the loading rate, the evolutions of the volumetric strain versus time are shown in Fig. 12. By observing the curves plotted in this figure, together with the loading rates given in Fig. 8, some preliminary comments can be drawn. It is evident that the higher the loading rate, the

higher is the induced volumetric strain rate $\dot{\varepsilon}_v$, defined as the tangent to the $\varepsilon_v - t$ curve. Furthermore, effect of yielding behaviour is also straightforward: for the same value of imposed loading rate, volumetric strain rate increases at yield due to plastic flow. It follows that for a pertinent analysis of the tests performed, a careful investigation of the induced volumetric strain rates is needed. This is done in Fig. 13 and it can be observed that change in volumetric strain rate for these tests occurs unconditionally at yield, sometimes passing from a loading phase to a creep phase. It is possible, however, to associate the change of the logarithmic linear fit of the volumetric strain versus time with the excess pore pressures generation. Considering, for instance, the branch of the curve of test T2 ($s = 0.2$ MPa; i.e. $S_{rw} \cong 30\%$, cf. Fig. 4) after the yield point (Fig. 13(b)), it is likely that the induced volumetric strain rate under a mean total stress $p$, which is continuously increasing, is equal to the volumetric strain rate during the first two creep phases, where $p$ is constant. Thus, one can imagine that no excess pore pressure, or at least the same amount of excess pore pressure, is developing in this phase. Oppositely, the passage from the second creep to reloading at fast rate induces a dramatic change in the volumetric strain rate, and this could be associated with excess pore pressure generation. Obviously, the opposite holds true; hence, the passage from a loading phase at fast rate to a creep phase gives rise to a change in the volumetric strain rate (Figs. 13(a) and (c)) associated with excess pore pressure dissipation.

In order to have an insight into the time-dependent behaviour of chalk, as observed from the results presented so far, evolutions of creep phases of Lixhe chalk at various suction levels and constant total mean stresses are summarised in Fig. 14. Results are presented in terms of volumetric strain versus time in log scale. Various trends are depicted; it can be observed that:

—for creep test at low stress levels (approximately when $p < 25$ MPa) volumetric strain curves increase continuously with time (Fig. 14(a) and first creep phases in Figs. 14(b) and (c));

—high stress levels change the shape of the curve, inducing at the beginning of the test a rapid increase in the volumetric strain (Figs. 14(a), (b) and (c));

—at same applied stress levels, the higher the suction, the lower is the amount of induced volumetric strain (Figs. 14(b) and (c), tests T2 and T4 at $p \cong 50$ MPa);

—the difference between the amount of volumetric strain generated during repeated creep phases seems to reduce increasing suction (tests T2 and T5, Figs. 14(b) and (c)).

From the shape of the curves in Fig. 14, it seems clear that only in two circumstances it is admissible to claim that effective creep began at constant mean net stress $p_{net}$ and constant suction (i.e. complete dissipation of excess pore-oil and pore-water pressures), namely: in test T5 (second creep, Fig. 14(b)) and in test T2 (third creep, Fig. 14(c)).

These tests have been analysed using the approach proposed by Janbu (1985). Results of the analysis of test

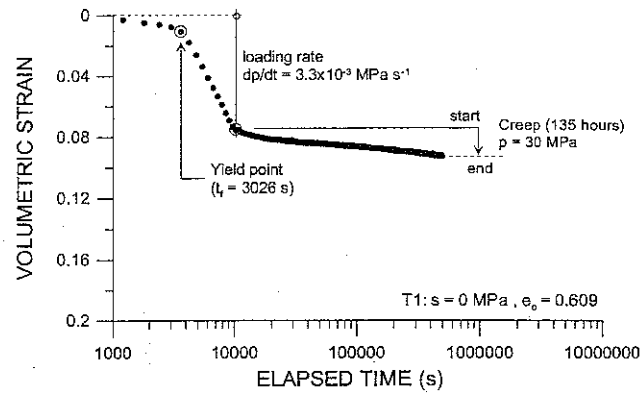


(a)

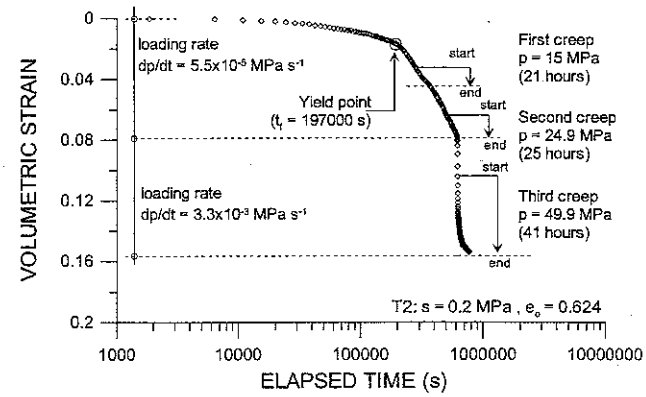


(b)

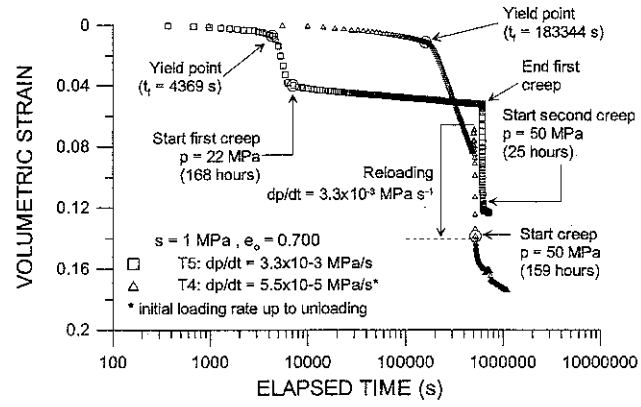


(c)

**Fig. 13. Volumetric strain variation for isotropic triaxial tests on Lixhe chalk at various suction levels: (a) $s = 0$ MPa, (b) $s = 0.5$ MPa and (c) $s = 1$ MPa**

T2 are presented in Fig. 15. Following Janbu's method, time $T_c$ for primary consolidation under constant load and time $T_p$ for complete dissipation of excess pore pressure are obtained by means of the coupled analysis of the evolution of the time resistance $R = \dot{\varepsilon}_v^{-1}$ and the volumetric strain versus time during a constant load step. The latter curves are plotted in Fig. 15 for the third creep of test T2. The two points corresponding to the end of the primary consolidation (time $T_c$) and the complete dissipation of excess pore pressure (time $T_p$) in test T2 are

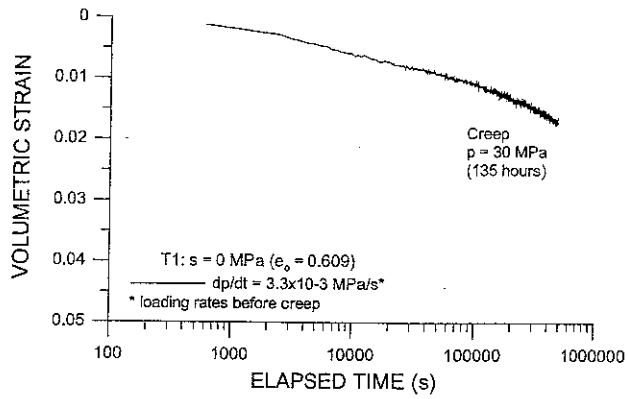


(a)

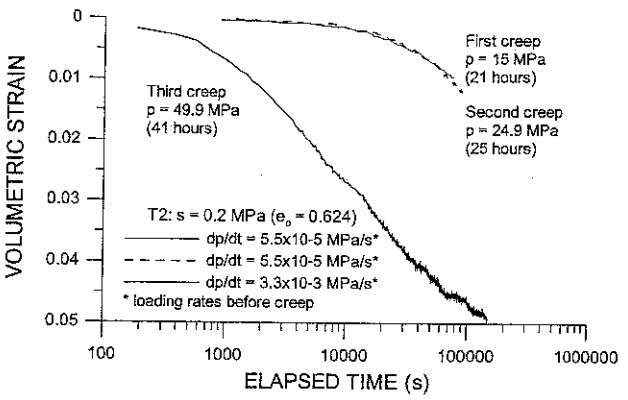


(b)

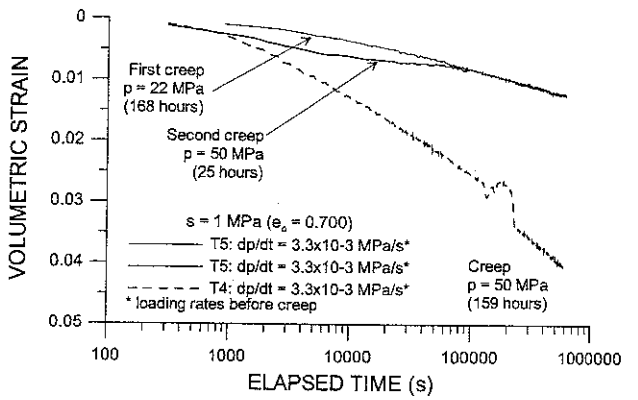


(c)

**Fig. 14. Creep phases on Lixhe chalk at various suction levels: (a) $s=0$ MPa, (b) $s=0.5$ MPa and (c) $s=1$ MPa**

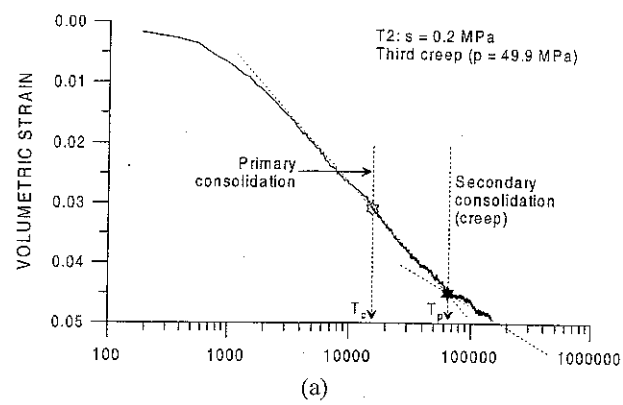


(a)

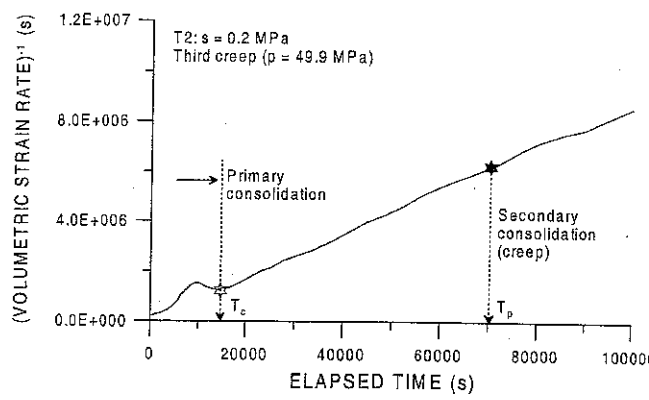


(b)

**Fig. 15. Analysis of creep phases for test T2**

sketched in the same figure. Since the analysis has been performed according to data coming from test T2 at $s=$ 0.2 MPa ($S_{rw} \cong 30\%$) and test T5 at $s=1$ MPa ($S_{rw} \cong 10\%$) one may wonder whether it is reasonable to consider this result independent of the suction level imposed during the test.

In order to verify this aspect, the characteristic points demonstrating for tests T2 and T5 the end of primary consolidation and the complete dissipation of pore pressure are plotted in a volumetric strain-strain rate semi-logarithm diagram, as shown in Fig. 16. The points corresponding to time $T_p$ for complete dissipation of excess pore pressure (bold symbol) allow identification of the maximum value of admissible volumetric strain rate for which the mean net stress $p_{net}=p-u_o$ is constant (i.e. $\Delta u_o \cong 0$). From the results shown in Fig. 16 it is possible to infer that, independently of the nature of the test (isotropic compression loading or creep), but depending on the imposed suction level, a maximum volumetric strain rate can be found for which tests can be still considered fully drained. Results from tests T2 ($s=0.2$ MPa) gives $\dot{\varepsilon}_v \lesssim 3 \times 10^{-7}\ s^{-1}$, whereas tests T5 ($s=1$ MPa) define a threshold for the volumetric strain rate of about $5 \times 10^{-8}\ s^{-1}$. It is worth noting that results relative to test T2 allow justifing the hypothesis of fully drained condition for this test during isotropic compression loading and up to the end of the second creep phase (Fig. 13(b)). The same conclusion can not be drawn for test T5, since apparently the induced volumetric strain rate exceeds the threshold $\dot{\varepsilon}_v = 5 \times 10^{-8}\ s^{-1}$ during isotropic compression loading at fast rate.

It is thought that one possible reason for this behaviour is associated with the difference existing in the dissipation process, depending on the nature of the interaction between the saturating fluids and the soil skeleton. Thus, the higher viscosity of Soltrol 170 and the disposition of

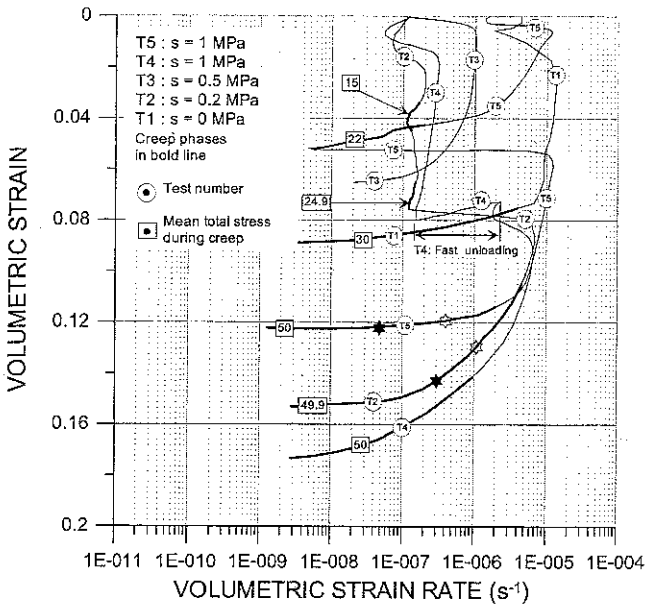


**Fig. 16. Volumetric strain-strain rate relationship during isotropic triaxial compression tests on Lixhe chalk**

chalk to be water-wet rather than oil-wet could explain the longer time for complete dissipation of excess pore pressure observed during test T5 at higher suction level (i.e. lower water saturation). Consequently, changes in $S_{rw}$ (i.e. change in suction) bear a different time for complete dissipation. The practical implications of this behaviour in chalk are relevant if related to the enhanced oil recovery procedure adopted in reservoir chalk, carried out usually by sea water injection (waterflooding). In this specific case, water saturation increase due to waterflooding causes increasing volumetric strain rate and a progressive early dominance of creep.

Moving from the analysis presented in this section, some additional comments can be drawn with respect to the results presented in Figs. 10 and 11. It is likely that the difference in bulk modulus and yield stress existing between the tests conducted at the two selected loading rates is essentially due to the difference between the fully drained strength mobilised in the tests run at slow rate and the undrained strength typical of the "fast" tests. There is no doubt, however, that for the same loading rate suction influences both bulk modulus and yield stress values (Figs. 10 and 11). Unfortunately, as already mentioned, we have enough data, related to yield mean total stress at low suction levels for chalk samples at $e_o \cong 0.7$. Hence, the $s-p$ relationship proposed in Fig. 11 (dot line) needs to be corroborated by further experimental results.

*Creep Effects: Apparent Preconsolidation Pressure, Stress Overshooting*

Among the recurrent observations associated with creep experiments, apparent preconsolidation pressure and stress overshooting are often mentioned. This type of behaviour has been deeply discussed by Tatsuoka et al. (2000), related to the post-creep undrained behaviour of Fujinomori clay.

The existence of such a behaviour for Lixhe chalk is confirmed by the results shown in Fig. 17, which give some details of the isotropic compression tests already presented in Fig. 9. During test T2 (Fig. 17(b)), performed at initial slow loading rate, a first creep phase of about 21 hours was allowed to develop after the yield point, under a constant mean total stress of 15 MPa. After that, a second loading phase at the same slow rate was run. As can be observed, the reloading curve rejoins the original initial loading curve without any temporary overshooting of the apparent preconsolidation stress. It is a type of behaviour very similar to the temporary strengthening of the links of the clay structure (Bjerrum, 1967), most geotechnical engineers might be aware of. Time effect could lead to the development of additional strength related to a chemo-mechanical coupling associated with the precipitation of cementing agents like calcite. The importance of chemistry on the mechanical behaviour of chalk has been recently emphasised by Hellmann and co-workers (Hellmann et al., 2002a; Hellmann et al., 2002b). Therefore, the results presented herein seem to corroborate the idea that chemistry could play an important role in characterising the time-dependent behaviour of chalk. After the reloading which follows the first creep phase, a second creep phase (at 24.9 MPa) and a new reloading at faster rate ($3.3 \times 10^{-3}$ MPa $s^{-1}$) were done. In this case, the response of the sample is quite different, and a clear overshooting of the apparent preconsolidation stress can be observed, associated with the fast loading rate and the consequent excess pore pressure. Finally, the reloading curve rejoins the original initial loading curve at higher stresses before the beginning of the third creep.

By comparison between test T2 and T5 (Figs. 17(b) and (c)), it is evident that the temporary increase of the apparent preconsolidation stress upon reloading after creep is essentially due to the excess pore pressure generated. This is corroborated by the results of test T4 (Fig. 17(c)), where the apparent preconsolidation stress overshooting follows an unloading phase. As a concluding remark, based on the values obtained for the coefficients of compressibility $C_c$, it is possible to recognise that the effect of the loading rate on the overall compressibility of the chalk seems to be negligible.

## CONSTITUTIVE MODELLING

The developed constitutive model (Pasachalk model) is a cap type plasticity model coupled with the Barcelona Basic Model (BBM) (Alonso et al., 1990) for taking the suction effect into account. As viscous effects may be important for the reservoir exploitation period, a first development of an elastoviscoplastic constitutive model is presented. The idea is to combine the framework of the Perzyna viscoplasticity (1964) with the elastoplastic BBM. In such a way, the yield surfaces of BBM become potential surfaces for the description of viscous effects,

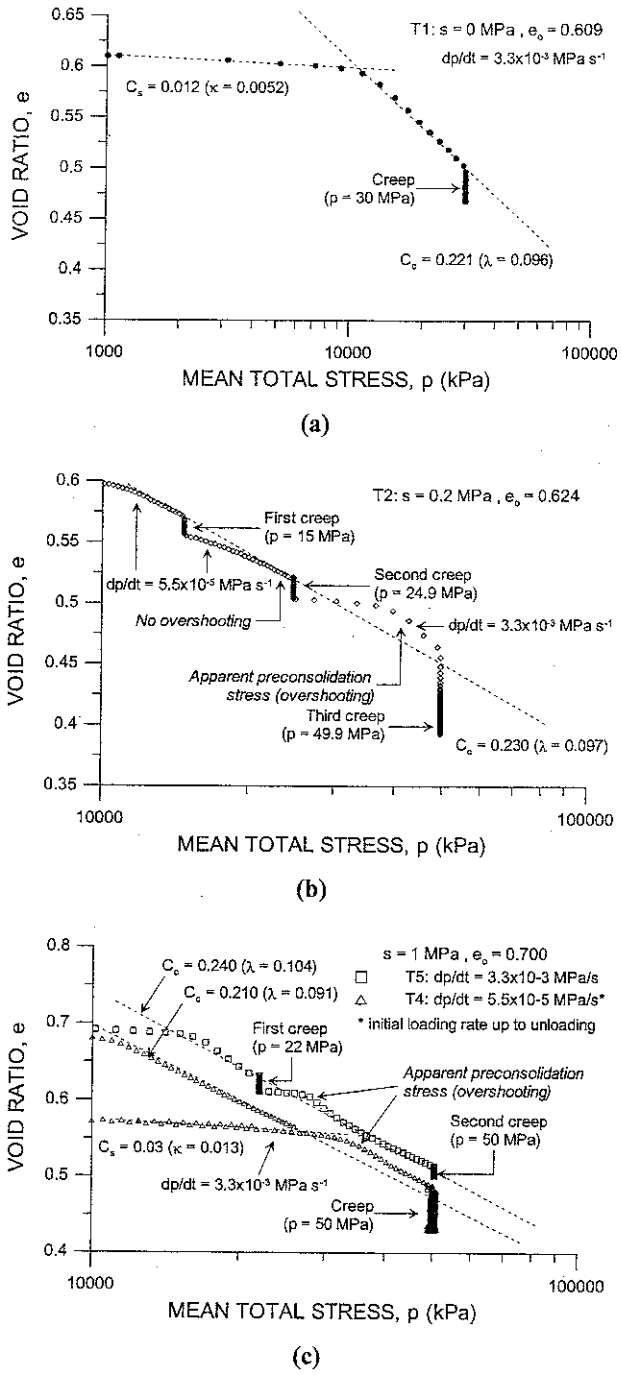


**Fig. 17. Details of isotropic compression tests on Lixhe chalk at various suction levels**

whose amplitude depends on the stress point distance to the potential surface. The elastoplastic basis of BBM is first presented. The modifications and extensions to the viscous strains modelling are then described, and a first application assessing the model capability is presented.

Previous experiments performed on chalk samples have shown two plastic mechanisms: the pore collapse for high mean stresses (contractant behaviour) and the frictional failure for low mean stresses. The pore collapse could be caused by the breakdown of physico-chemical bonds between the grains inducing some grain-to-grain slip (Monjoie et al., 1990). The frictional failure corresponds to a plastic distortion inducing an increase of porosity. These two plastic mechanisms are modeled by two yield surfaces combined within a cap model: the modified Cam-Clay model is used for pore collapse whereas an internal friction model for friction failure. Since experimental results show that the chalk strength under extension can be overestimated using an internal friction model, a third yield surface is adopted to limit the traction stresses. These surfaces will be specified in the next sections.

As far as the suction effect is concerned, the model adopts the approach developed in the BBM where the suction is considered as an independent variable that modifies yield surfaces and produces reversible and irreversible deformations.

*Mechanical Elastoplastic Model (Pasachalk Model)*

The mechanical model is expressed in terms of the following stress invariants and the suction:

$$I_\sigma = \sigma_{ii} \tag{2}$$

$$II_{\hat{\sigma}} = \sqrt{\frac{1}{2}\hat{\sigma}_{ij}\hat{\sigma}_{ij}}, \quad \hat{\sigma}_{ij} = \sigma_{ij} - \frac{I_\sigma}{3}\delta_{ij} \tag{3}$$

$$III_{\hat{\sigma}} = \frac{1}{3}\hat{\sigma}_{ij}\hat{\sigma}_{jk}\hat{\sigma}_{ki} \tag{4}$$

$$\beta = -\frac{1}{3}\sin^{-1}\left(\frac{3\sqrt{3}}{2}\frac{III_{\hat{\sigma}}}{II_{\hat{\sigma}}^3}\right) \tag{5}$$

$$s = u_o - u_w. \tag{6}$$

Where $\beta$ is the Lode angle, $s$ is the suction, and $u_o$ and $u_w$ are the oil and water pressures, respectively.

Following the additivity postulate, the strain rate is composed of a mechanical part (superscript $m$) and a suction one (superscript $s$). Each contribution is partitioned in an elastic (superscript $e$) and a plastic component (superscript $p$):

$$\dot{\varepsilon}_{ij} = \dot{\varepsilon}_{ij}^{m,e} + \dot{\varepsilon}_{ij}^{s,e} + \dot{\varepsilon}_{ij}^{m,p} + \dot{\varepsilon}_{ij}^{s,p}. \tag{7}$$

Hooke's elasticity is assumed for the mechanical elastic part:

$$\dot{\sigma}_{kl} = C_{klij}^{e}\dot{\varepsilon}_{ij}^{m,e} \tag{8}$$

where $C^e$ is the compliance elastic tensor. For the plastic part, a general framework of non-associated plasticity is adopted in order to limit dilatancy. In that case, the plastic flow rate is derived from a plastic potential $g_\alpha$:

$$\dot{\varepsilon}_{ij}^{m,p} = \dot{\lambda}^p \frac{\partial g_\alpha}{\partial \sigma_{ij}}, \tag{9}$$

where $\lambda^p$ is a scalar multiplier and $g_\alpha$ is the plastic potential related to the plastic mechanism $\alpha$. Elastic and plastic strains related to suction changes are defined following BBM expressions. Irreversible strains are induced when the suction becomes higher than a suction level $s_o$, they are as follows:

$$\dot{\varepsilon}_{ij}^{s,e} = \frac{\kappa_s}{(1+e)}\frac{\dot{s}}{(s+p_{at})}\delta_{ij} = h_{ij}^{e}\dot{s} \tag{10}$$

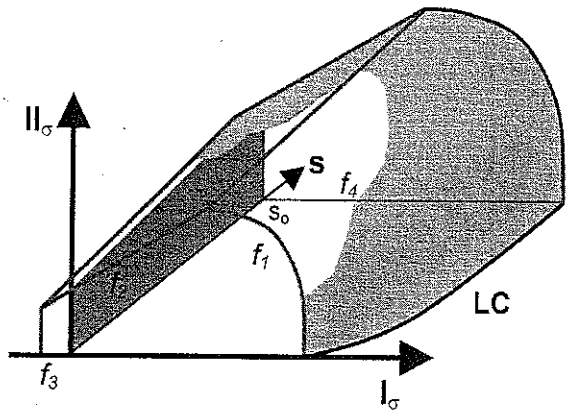


**Fig. 18. Yield surfaces of Pasachalk model in the stress space**

$$\dot{\varepsilon}_{ij}^{s,p} = \frac{\lambda_s - \kappa_s}{(1+e)} \frac{\dot{s}}{(s+p_{at})} \delta_{ij} = h_{ij}^{p} \dot{s}. \tag{11}$$

Where $e$ is the void ratio, $p_{at}$ is the atmospheric pressure, $\kappa_s$ and $\lambda_s$ are elastic and plastic coefficients. The Eqs. (7) and (8) can be rewritten as:

$$\dot{\sigma}_{kl} = C_{klij}^{e} \left( \dot{\varepsilon}_{ij} - h_{ij}^{e} \dot{s} - \lambda^{p} \frac{\partial g_\alpha}{\partial \sigma_{ij}} - h_{ij}^{p} \dot{s} \right). \tag{12}$$

Considering a general hardening/softening plastic law depending on the internal variable $\zeta$, the consistency condition related to the yield function $f_\alpha$ can be formulated as:

$$\dot{f}_\alpha = \frac{\partial f_\alpha}{\partial \sigma_{ij}} \dot{\sigma}_{ij} + \frac{\partial f_\alpha}{\partial_s} \dot{s} + \frac{\partial f_\alpha}{\partial \zeta} \dot{\zeta} = 0. \tag{13}$$

Substituting (12) in (13), the expression of multiplier $\lambda^p$ can be found and the stress rate can be computed:

$$\dot{\sigma}_{kl} = (C_{klij}^{e} - C_{klij}^{p}) \dot{\varepsilon}_{ij} - M_{kl} \dot{s}. \tag{14}$$

The first term of the right side is the classical expression of an elastoplastic formulation. The second term is related to the suction.

Cam-Clay pore collapse model

The Cam-Clay yield surface is defined by the following expression (Fig. 18):

$$f_1 \equiv II_{\hat{\sigma}}^2 + m^2 \left( I_\sigma + \frac{3c}{\tan \phi_c} \right) (I_\sigma - 3p_0) = 0 \tag{15}$$

where $c$ is the cohesion, $\phi_C$ is the friction angle in compression path, $p_o$ is the preconsolidation pressure which defines the size of the yield surface, and $m$ is a coefficient introduced to take into account the effect of the third stress invariant. The coefficient $m$ is defined by:

$$m = a(1 + b \sin 3\beta)^n \tag{16}$$

where the parameters $a$, $b$ and $n$ must verify some convexity conditions (Van Eekelen, 1980). Assuming associated plastic flow, the preconsolidation pressure $p_o$ is related to the volumetric plastic strain $d\varepsilon_v^p$ following the kinematic equation:

$$dp_0 = \frac{1+e}{\lambda - \kappa} p_0 d\varepsilon_v^p, \tag{17}$$

where $\lambda$ is the compression coefficient and $\kappa$ is the elastic coefficient.

Expression (17) allows accounting for both hardening or softening according to the sign of the volumetric plastic strain. However, in the cap model, the softening zone will not be considered. On the other hand, it should be noted that the irreversible volumetric strain includes the coupled effect of mechanical and suction changes.

Internal friction model

In order to formulate a friction model based on a Mohr-Coulomb type failure criterion with a smoothed plastic surface, the Van Eekelen's (1980) formulation has been used. The latter is based on a modification of the Drucker-Prager's failure cone, by introducing a dependence on the Lode's angle $\beta$. With this assumptions, the failure criterion can be written as:

$$f_2 \equiv II_{\hat{\sigma}} - m \left( I_\sigma + \frac{3c}{\tan \phi_C} \right) = 0. \tag{18}$$

As for the cap model (Cam-Clay), non-associated plasticity is considered also for the friction model (Fig. 18), using a plastic potential definition similar to Eq. (18), where the dilatancy angle $\psi$ is used instead of the frictional angle $\phi_C$.

The evolution of the failure criterion is governed by the internal variables $\phi_c$ (friction angle for compression paths), $\phi_E$ (friction angle for extension paths) and $c$ (cohesion), following hardening relations:

$$\begin{aligned} \phi_C &= \phi_{C0} + \frac{(\phi_{Cf} - \phi_{C0})\, \varepsilon_{eq}^p}{B_p + \varepsilon_{eq}^p} \\ \phi_E &= \phi_{E0} + \frac{(\phi_{Ef} - \phi_{E0})\, \varepsilon_{eq}^p}{B_p + \varepsilon_{eq}^p} \\ c &= c_0 + \frac{(c_f - c_0)\, \varepsilon_{eq}^p}{B_c + \varepsilon_{eq}^p} \end{aligned} \tag{19}$$

where subscripts 0 and $f$ mean the initial and the final value respectively; $B_p$ and $B_c$ are parameters defining the value of plastic strains for which half of the value of the internal hardening variable is achieved. Equations (19) are a function of the cumulated equivalent deviatoric plastic strains $\varepsilon_{eq}^p$ during time $t$.

Suction effect on yield surface (BBM model)

Several phenomena are usually evident for unsaturated soils:

—The preconsolidation pressure $p_o$ and the material stiffness increase with suction. In BBM this is described by the LC curve, defined by the following expression:

$$p_0(s) = p_c \left( \frac{p_0^*}{p_c} \right)^{(\lambda(0)-\kappa)/(\lambda(s)-\kappa)} \tag{20}$$

with

$$\lambda(s) = \lambda(0)[(1-r) \exp(-\beta' s) + r] \tag{21}$$

where $p_0^*$ is the preconsolidation pressure for $s = 0$, $p_c$ is a reference pressure, $\lambda(0)$ is the compression coefficient at

zero suction, $\lambda(s)$ is the compression coefficient at suction $s$, $r$ is a parameter representing the maximum stiffness of the chalk, and $\beta'$ is a parameter controlling the stiffness increase with suction increase.

—Cohesion increases with suction, this is modelled using Eq. (22). The influence of suction on friction angle depends on the material studied. Experiment on chalk shows that friction angle is independent of the saturating fluid.

$$c(s) = c(0) + ks \tag{22}$$

where $k$ is a material constant, $c(0)$ is the cohesion at saturated state.

—Suction changes may create irreversible strains. In the BBM model, this is modelled thanks to a yield surface, the SI "Suction Increase" curve. When suction becomes higher than a suction level $s_0$, plastic strains are created (Fig. 18). This yield criterion is introduced in our constitutive law:

$$f_4 \equiv s - s_0 = 0. \tag{23}$$

*Mechanical Elastoviscoplastic Model*

As it has been shown, viscous effects in chalk may be relevant during triaxial tests performed at various stress rates and involving creep stages. Time-dependent behaviour modelling of fully saturated chalk is here introduced based on the elastoviscoplastic approach proposed by Perzyna (1964). The major advantage of such an approach is the possibility to formulate the elastoviscoplastic model moving directly from the general theoretical structure of the elastoplastic one (Pasachalk model). Besides, the Perzyna's elastoviscoplastic theory has been adopted also because:

—the formulation is well accepted and well used;

—the generality of the time-rate flow rule offers the capability of simulating time-dependent behaviour over a wide range of loading;

—it gives a possibility to take advantage of the non-viscous multisurface cap-failure-tension model, developed for elastoplastic modelling;

—the formulation is readily adaptable to a numerical algorithm suitable for finite element procedure.

Hence, the strains are divided in reversible and irreversible parts:

$$\dot{\underline{\varepsilon}} = \dot{\underline{\varepsilon}}^{e} + \dot{\underline{\varepsilon}}^{vp} \tag{24}$$

$$\dot{\underline{\sigma}} = \underline{\underline{C}}^{e}(\dot{\underline{\varepsilon}} - \dot{\underline{\varepsilon}}^{vp}). \tag{25}$$

The irreversible strain may be described as normal to some potential $g$:

$$\dot{\underline{\varepsilon}}^{vp} = \gamma \langle \phi(f) \rangle \frac{\partial g}{\partial \underline{\sigma}}. \tag{26}$$

This formulation is rather similar to the elastoplastic one, but it is not based on the consistency condition. The amount of strain rate is described with respect to a reference surface $f$, similar to the yield surface. Then, we may define two irreversible mechanisms, one dedicated to the pore collapse, the second to the friction failure.

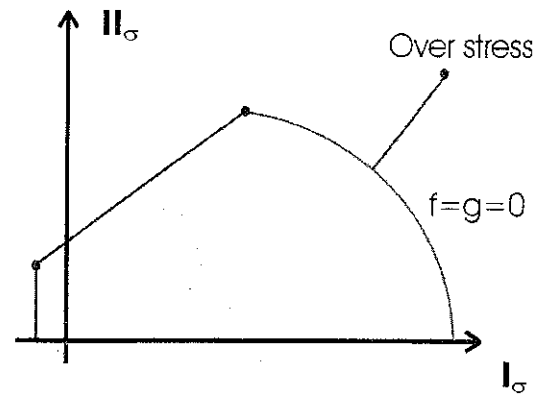


**Fig. 19. Over stress state and reference yield surface**

The pore collapse is based on the following equations:

$$\langle \phi_c(f_c) \rangle = \left( \frac{f_c}{3p_0^2} \right)^{\alpha_c} \tag{27}$$

and (Shao et al., 1993):

$$f_c = \omega \left( \frac{I_\sigma}{p_a} \right)^1 \tag{28}$$

where the reference surface $f_c$ is similar to the yield surface of the Pasachalk model (15). The function $f_c$ may here be analysed as an overstress, or a measure of the amount of the stress state going outside the yield or reference surface. Moreover, the overstress is only positive when the stress state is outside the yield—reference surface (Fig. 19). As the Macaulay's brackets are used in Eqs. (26) and (27), the irreversible strains exist only in this peculiar situation. The more the overstress, the more is the irreversible strain rate. Obviously, a hardening rule has to be defined, and the plastic hardening rule (17) is here adopted. For the friction failure, a similar development may be considered and implemented without major difficulties.

*Numerical Results*

As a preliminary remark, it should be emphasised that suction effects are not accounted for in the present version of the elastoviscoplastic model. Consequently, the numerical results shown in this section will concern experimental results obtained on fully saturated chalk at high suction levels (e.g. $s = 1$ MPa, Fig. 4). Indeed, for this condition it is admitted that chalk samples have essentially a "oil-like" behaviour. Viscous effects are then associated principally to oil-skeleton interactions. For the sake of brevity results related to "water-like" behaviour, published elsewhere (Charlier et al., 2002), are not considered here.

Figure 20 show isotropic compression experimental results and the proposed constitutive model responses for oil saturated chalk. Test T4 (Figs. 9 and 13(c)) has been reproduced using Soltrol saturated chalk parameters and accounts for both elastoplastic and elastoviscoplastic behaviour. Model parameters are summarised in Table 3.

In a first attempt, only the elastoplastic response was

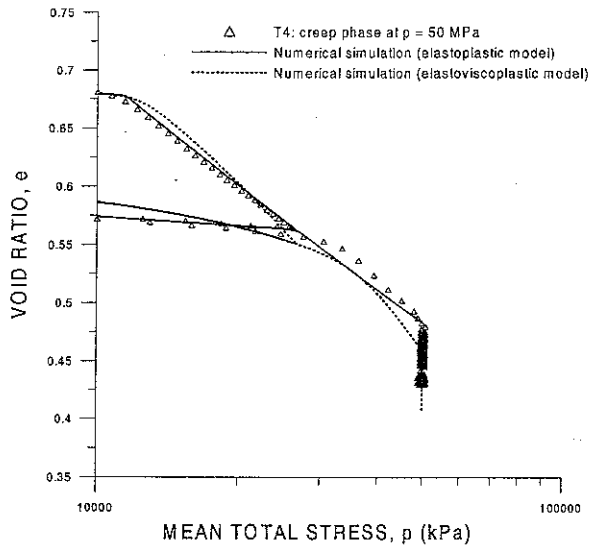


Fig. 20. Isotropic compression test on almost oil saturated Lixhe chalk ($S_{rw} \cong 10\%$): numerical versus experimental results

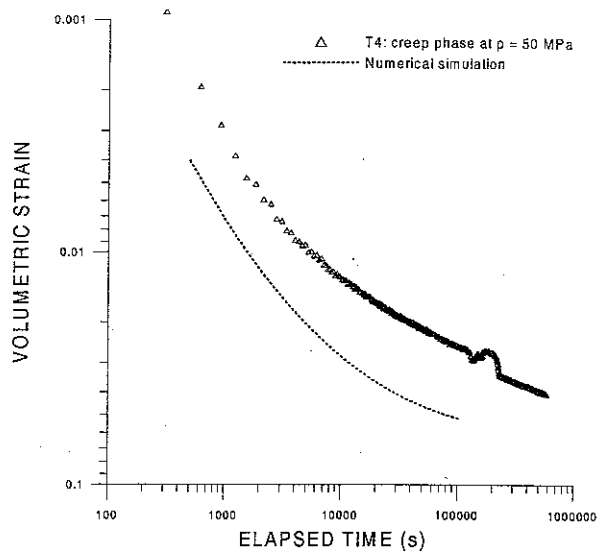


Fig. 21. Creep test on almost oil saturated Lixhe chalk ($S_{rw} \cong 10\%$): numerical versus experimental results

Table 3. Model parameters

| Parameters of the elastoplastic model | | | |
|---|---|---|---|
| Linear elasticity | Parameter | Value | Unit |
| | $E$ | 1.48 | GPa |
| | $\nu$ | 0.177 | — |
| Frictional mechanism | | | |
| | $\phi_E = \phi_C$ | 28.2 | ○ |
| | $\psi_E = \psi_C$ | 0 | ○ |
| | $c$ | 1.61 | MPa |
| Cam Clay + suction LC | | | |
| | $p_o$ | 11.3 | MPa |
| | $\lambda(0)$ | 0.18 | — |
| | $r$ | 0.95 | — |
| | $\beta'$ | 8.0 | $MPa^{-1}$ |
| | $p_c$ | $3 \times 10^{-3}$ | MPa |
| Parameters of the elastoviscoplastic model | | | |
| Hardening parameter | $E_{cro}$ | 0.05 | — |
| Viscosity parameter | $\alpha_c$ | 9.9 | — |
| Viscosity parameter | $\omega$ | $5.1 \times 10^{-8}$ | — |
| Viscosity parameter | $\tau$ | 0 | — |

considered. This allowed the calibration of Pasachalk model parameters in view of an elastoviscoplastic modelling of chalk behaviour. Consequently, neither apparent preconsolidation overshooting nor creep were simulated. However, both elastic response and yield (preconsolidation) were well captured by the elastoplastic model.

Results obtained introducing viscous effects are presented in the same figure. As can be observed, either apparent preconsolidation overshooting and creep can be simulated adopting a viscoplastic approach. Results of simulations are in good agreement with the experimental ones, though the elastoviscoplastic model tends to slightly overestimate chalk compressibility for mean total stress values higher than 20 MPa (Fig. 20). Figure 21 presents the evolution of volumetric strain during the creep phase at 50 MPa. Again, model results compare qualitatively well with the experimental measurements.

## CONCLUSIONS

The problem of the stress-strain time-dependent behaviour of a multiphase saturated chalk has been presented in this paper. Moving from the hypothesis that the mechanical behaviour of a chalk full of oil and water can be described within the same theoretical framework of unsaturated soils, the relevant developments allowing for chalk mechanical testing under oil-water suction control have been described. The results of an experimental study investigating the behaviour of chalk under isotropic triaxial compression and controlled suction conditions have been discussed. Osmotic technique and overpressure technique were used to control suction. Their compatibility in controlling suction in chalk was verified. It was recognised that oil-water suction influences the mechanical response of the material. Increasing suction levels induce stiffer response in the elastic regime, increase the mean total stress at yield and lead to a more pronounced transition from elastic to elastoplastic regime when yield occurs. As far as time-dependent behaviour is concerned, both effects of loading rate and creep were considered. The effect of loading rate was analysed with regards to the relevant induced volumetric strain rate, in order to assess conditions corresponding to fully drained mechanical testing. The analysis of creep phases under controlled suction conditions indicates that suction influences the evolution of creep. In particular, it was observed that suction decrease causes increasing volumetric strain rate and a progressive early dominance of creep over primary consolidation. Numerical modelling of the mechanical behaviour of Lixhe chalk was proposed. The response predicted by the model seems to fit well the experimental

results and the basic features of the time-dependent phenomena. An enhanced version of the model accounting for suction effects is foreseen.

## ACKNOWLEDGEMENTS

The results presented in this paper have been obtained within the framework of the European project PASACHALK 2 (contract n° ENK6-2000-00089) carried out jointly by the University of Liege (Dpt. GeomaC, Belgium), the Ecole Nationale des Ponts et Chaussées (ENPC, Dpt. CERMES, Paris, France) and TotaFinaElf oil company (Drs, Ph. Keul and A. Onaisi). The precious collaboration of A. Avagnina (double diploma, Politecnico di Torino and ENPC Paris) and A. Linares Gomez (Erasmus program, Universitat Politecnica de Catalunya a Barcelona) is also acknowledged.

## REFERENCES

1) Adachi, T. and Oka, F. (1982): Constitutive equations for normally consolidated clays based on elasto-viscoplasticity, *Soils and Foundations*, **22**(4), 57–70.
2) Alonso, E. E., Gens, A. and Josa, A. (1990): A constitutive model for partially saturated soils, *Géotechnique*, **40**(3), 405–430.
3) Andersen, M. A., Foged, N. and Pedersen, H. F. (1992): The link between waterflood-induced compaction and rate-sensitive behavior in a weak north sea chalk, *4th North Sea Chalk Symposium*, Deauville, France.
4) Andersen, M. A. (1995): Petroleum research in north sea chalk. Public, *Rogaland Research*, Stavanger, Norway.
5) Bishop, A. W. and Donald, I. B. (1961): The experimental study of partly saturated soil in the triaxial apparatus, *Proc. 5th ICSMFE*, **1**, 13–21.
6) Bjerrum, L. (1967): Engineering geology of Norwegian normally-consolidated marine clays as related to settlement of buildings, *Géotechnique*, **17**, 81–118.
7) Charlier, R., Collin, F., Schroeder, Ch., Illing, P., Delage, P., Cui, Y.-J. and De Gennaro, V. (2002): Constitutive modeling of chalk-application to waterflooding, *Proc. 2nd Biot Conference*, Grenoble, France (in print).
8) Collin, F., Cui, Y.-J., Schroeder, Ch. and Charlier, R. (2002): Mechanical behaviour of Lixhe chalk partly saturated by oil and water: experiment and modeling, *Int. J. for Num. Anal. Meth. in Geomechanics*, **26**, 897–924.
9) Cui, Y. J. and Delage, P. (1996): Yielding and plastic behaviour of an unsaturated compacted silt, *Géotechnique*, **46**(2), 291–311.
10) Delage, P., Suraj de Silva, G. P. R. and De Laure, E. (1987): Un nouvel appareil triaxial pour les sols non saturés, *9th Eur. Conf. of Soil Mechanics*, Dublin, 26–28.
11) Delage, P., Suraj de Silva, G. P. R. and Vicol, T. (1992): Suction controlled testing of non saturated soils with an osmotic consolidometer, *Proc. 7th Int. Conf. on Expansive Soils*, Dallas, 206–211.
12) Delage, P., Schroeder, Ch. and Cui, Y.-J. (1996): Subsidence and capillary effects in chalk, *Proc. Eurock 96*, Turin, 1291–1298.
13) Delage, P., Howat, M. and Cui, Y.-J. (1998): The relationship between suction and swelling properties in a heavily compacted unsaturated clay, *Engrg. Geology*, (50)1-2, 31–48.
14) Gibson, R. E. and Henkel, D. J. (1954): Influence of duration of tests at constant rate of strain on measured "drained" strength, *Géotechnique*, **4**(1), 6–15.
15) Graham, J., Crooks, J. H. A. and Bell, A. L. (1983): Time effects on the stress-strain behaviour of natural soft clays, *Géotechnique*, **33**(3), 327–340.
16) Gutierrez, M. and Kolderup, U. M. (1999): Joint Chalk Reasearch Phase V. Modelling time-dependent chalk behaviour and chalk-water interaction, Draft report no. 541105-4 (NGI).
17) Havmøller, O. and Foged, N. (1998): Confidential report DGI.
18) Hellmann, R., Renders, P. J. N., Gratier, J.-P. and Guiguet, R. (2002a): Experimental pressure solution compaction of chalk in aqueous solutions. Part 1. Deformation behaviour and chemistry, *Water-Rock Interactions, Ore Deposits, and Environmental Geochemistry: A Tribute to David A. Crerar; The Geochemical Soc.* (eds. by Hellmann and Wood), Special Publication (7), 129–152.
19) Hellmann, R., Gaviglio, P., Renders, P. J. N., Gratier, J.-P., Békri, S. and Adler, P. (2002b): Experimental pressure solution compaction of chalk in aqueous solutions. Part 2. Deformation examined by SEM, porosimetry, synthetic permeability and X-ray computerized tomography, *Water-Rock Interactions, Ore Deposits, and Environmental Geochemistry: A Tribute to David A. Crerar; The Geochemical Soc.* (eds. by Hellmann and Wood), Special Publication (7), 153–178.
20) Hermansen, H., Landa, G. H., Sylte, J. E. and Thomas, L. K. (2000): Experiences after 10 years of waterflooding the Ekofisk Field, Norway. *J. of Petroleum Science and Eng.*, **26**, 11–18.
21) Ho, D. Y. and Fredlund, D. G. (1982): Strain rates for unsaturated soil shear strain testing. *Proc. 7th South-East Asia Conf. SMFE*, Hong-Kong, 787–803.
22) Homand, S. and Shao, J. F. (2000): Mechanical behaviour of a porous chalk and effect of saturating fluid, *Int. J. of Mechanics of Cohesive-Frictional Materials*, **5**, 583–606.
23) Janbu, N. (1985): Soil models in offshore engineering, 25th Rankine Lecture. *Géotechnique*, **35**(3), 241–281.
24) Kassif, G. and Ben Shalom, A. (1971): Experimental relationship between swell pressure and suction, *Géotechnique*, **21**(3), 245–255.
25) Krogsbøll, A. (1997): Simultaneous consolidation and creep, *Int. Symp. on Modelling in Soil Mechanics*, Technical University of Denmark, Lyngby, Denmark.
26) Leroueil, S., Kabbaj, M., Tavenas, F. and Bouchard, R. (1985): Stress-strain-strain rate relation for compressibility of sensitive natural clays, *Géotechnique*, **35**(2), 159–180.
27) Mancuso, C., Vassallo, R. and D'Onofrio, A. (2002): Small strain behaviour of a silty sand in controlled-suction resonant column-torsional shear tests, *Can. Geotech. J.*, **39**, 22–31.
28) Monjoie, A., Schroeder, Ch., Da Silva, F., Debande, G., Detiège, Cl. and Poot, B. (1985): Characterisation and inhibition of chalks, *North Sea Chalk Symp.*, Stavanger, Norway.
29) Morrow, N. R. (1970): Physics and thermodynamics of capillary, *Industrial and Engrg. Chemistry*, **62**(6), 32–56.
30) Nagel, N. (2001): Ekofisk geomechanics monitoring, *Int. Workshop on Geomechanics in Reservoir Simulation*, IFP, Reuil-Malmaison, France.
31) Newman, G. H. (1983): The effect of water chemistry on the laboratory compression and permeability characteristics of some North Sea chalks, *J. of Petroleum Eng.*, 976–980.
32) Papamichos, E., Brignoli, M. and Santarelli, F. J. (1997): An experimental and theoretical study of partially saturated collapsible rock, *Int. J. of Mechanics of Cohesive-Frictional Materials*, **2**, 251–278.
33) PASACHALK (2000): Mechanical behaviour of partially and multiphase saturated chalks-fluid-skeleton interaction: main factor of chalk oil reservoirs compaction and related subsidence, *Final Report*, Contract EC no. JOF3CT970033.
34) Perzyna, P. (1964): The constitutive equations for rate sensitive plastic materials, *Quart. Appl. Mech.*, **20**, 321–332.
35) Piau, J. M. and Maury, V. (1994): Mechanical effects of water injection on chalk reservoirs, *Paper SPE/ISRM 28133*, EUROCK 1994.
36) Richards, L. A. (1941): A pressure-membrane extraction apparatus for soil solution, *Soil Science*, **51**, 377–386.
37) Richardson, A. M. and Whitman, R. V. (1963): Effect of the strain-rate upon undrained shear resistance of a saturated remoulded fat clay, *Géotechnique*, **13**, 310–324.
38) Risnes, R., Korsnes, R. I. and Vatne, T. A. (1999): Tensional

strength of soft chalks measured in direct and Brazilan tests, *Proc. 9th Int. Congr. ISRM*, 667–672.

39) Ruddy, I., Andersen, M. A., Pattillo, P. D., Bishlawi, M. and Foged, N. (1989): Rock compressibility, compaction and subsidence in a high porosity chalk reservoir: a case study of Valhall Field, *J. of Petroleum Technology*, **41**(7), 741–746.

40) Schroeder, Ch., Bois, A. P., Maury, V. and Halle, G. (1998): Water/chalk (or collapsible soil) interaction: Part II. Results of tests performed in laboratory on Lixhe chalk to calibrate water/chalk models, *SPE/ISRM (SPE 47587)*, Eurock'98, Trondheim.

41) Singh, A. and Mitchell, J. K. (1968): General stress-strain-time-function for soils, *J. Soil Mech. Div.*, ASCE, SM1, 21–45.

42) Tatsuoka, F., Santucci de Magistris, F., Hayano, K., Koseki, J. and Momoya, Y. (2000): Some new aspects of time effects on the stress-strain behaviour of stiff geomaterials, *Proc. Int. Conf. on the Geotechnics of HardSoils-Soft Rocks*, 1285–1371.

43) Williams, J. and Shaykewich, C. F. (1969): An evaluation of polyethylene glycol PEG 6000 and PEG 20000 in the osmotic control of soil water matric potential, *Can. Geotech. J.*, **102**(6), 394–398.